analytical chemistry

ARTICLE

pubs.acs.org/ac

Electrodialytic Membrane Suppressors for Ion Chromatography Make Programmable Buffer Generators

Yongjing Chen,[†] Kannan Srinivasan,[‡] and Purnendu K. Dasgupta*[,†]

[†]Department of Chemistry and Biochemistry, University of Texas at Arlington, Arlington, Texas 76019-0065, United States

[‡]Thermo Fisher Scientific, 445 Lakeside Drive, Sunnyvale, California 94085, United States

Supporting Information

ABSTRACT: The use of buffer solutions is immensely important in a great variety of disciplines. The generation of continuous pH gradients in flow systems plays an important role in the chromatographic separation of proteins, high-throughput pK_a determinations, etc. We demonstrate here that electrodialytic membrane suppressors used in ion chromatography can be used to generate buffers. The generated pH, computed from first principles, agrees well with measured values. We demonstrate the generation of phosphate and citrate buffers using a cation-exchange membrane (CEM) -based anion suppressor and Tris and ethylenediamine buffers using an anion-exchange membrane (AEM) -based cation suppressor. Using a mixture of phosphate, citrate, and borate as the buffering ions and using a CEM suppressor, we demonstrate the generation of a highly reproducible (avg RSD 0.20%, n = 3), temporally linear (pH 3.0−11.9, r^2 > 0.9996), electrically controlled pH gradient. With butylamine and a large concentration (0.5 M) of added NaCl, we demonstrate a similar linear pH gradient of large range with a near-constant ionic strength. We believe that this approach will be of value for the generation of eluents in the separation of proteins and other biomolecules and in online process titrations.

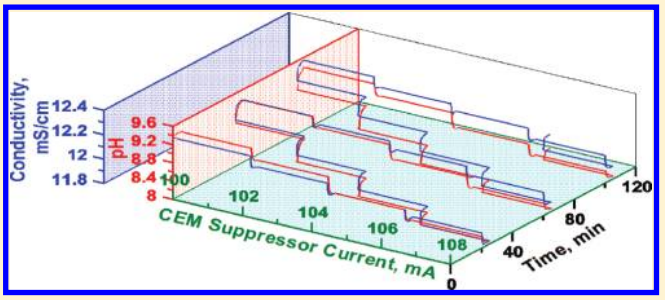

Buffers are of paramount importance in chemistry and biology. Buffers resist the change in activity/concentration of a specific ion when agents that would otherwise affect its concentration are added (or removed, e.g., by precipitation or volatilization). While the term usually refers to pH buffers, metal ion buffers are also in common use. In most living systems, buffering mechanisms exist to control pH within tight limits; the pH of each (sub)cellular compartment is precisely controlled.[1,2] Similar pH control is needed in myriad other processes, for example, in organic syntheses, where a pH electrode is used for pH measurement and constitutes part of a feedback system to add acid or base to maintain the pH at a preset level.[3] The use of such pH-stats is so common in biochemistry that 50+ year old reviews exist.[4] It has also long been realized that a constant pH can be maintained by electrochemically generating H^+ or OH^- in situ, rather than physically adding acid or base. For feedback, the pH can be measured directly by a pH electrode[5] (or better, after appropriate electrical isolation[6]) or photometrically via an indicator.[7] Many enzymatic reactions generate acid or base. The amount of electrochemically generated base or acid needed to maintain a constant pH is then coulometrically monitored. More recently, Gratzl and co-workers[8] demonstrated the ability to carry this out in a single 20 μL hemispherical drop as the reactor.

In biology/biochemistry, buffers based on phosphate, tris(hydroxymethyl)aminomethane (Tris), and citrate are among the most common. From capillary electrophoresis[9] to microbial fuel cells,[10] where H^+ and OH^- are electrolytically generated at the electrodes, consistent performance cannot be obtained without buffers.

For the present paper, the use of buffers as eluent components in liquid chromatography (LC) is of interest. Virtually all bioanalytes are ionizable; the degree of ionization controls chromatographic retention.[11,12] Even small changes in eluent pH and ionic strength (in addition to organic solvent content) can dramatically affect retention and efficiency, thus affecting the selectivity, peak shape, resolution, and reproducibility.[13] Measuring pH in mixed hydroorganic solvents is problematic. Theoretical computations are not straightforward and are typically of limited value.[14,15] The merit of pH-gradient liquid chromatography, with[16,17] or without[18,19] a concurrent solvent gradient, has recently been highlighted in a series of remarkable papers by Kaliszan et al. A theoretical framework has been constructed;[20] it has been shown that pK_a values of analytes can be obtained by such a technique.[21]

Ion-exchange chromatography of proteins has also long relied on buffers and pH gradients. A linear mobile phase pH gradient with a weak anion-exchanger stationary phase was termed *chromatofocusing*;[22,23] proteins elute in the order of their pI values. This has also been demonstrated in the capillary scale.[24] Concave and convex pH gradients may also have merit.[25]

Received: September 7, 2011
Accepted: November 21, 2011
Published: November 21, 2011

   dx.doi.org/10.1021/ac2023712 | *Anal. Chem.* 2012, 84, 67–75

pH gradient separations with low MW buffers have been pursued,[26,27] and attractive separations of monoclonal antibodies have been demonstrated.[28] Both pH and buffer concentrations have a profound effect.[29,30] Mobile-phase pH gradients are typically generated by blending different solutions. Both pH and buffer concentration cannot generally be independently varied.

Electrochemical pH-Stats versus Electrodialytic Membrane Suppressors in Ion Chromatography. Manipulations of pH by electrolysis as carried out in the electrochemical pH-stats result in electrolytic gas evolution. Depending on the specific experimental system, this may or may not be detrimental. In electrodialytically induced ion exchange or acid/base introduction, evolved gases can be isolated from the fluid of interest. The best known embodiment of this is the dual membrane suppressor used in ion chromatography (IC).[31,32] In a typical application, an eluent MX flows in a central channel bounded by two cation-exchange membranes (CEMs) and water flows on the exterior of each CEM. With an electrode placed in each outer channel, the M^+ ion (typically K^+ or Na^+) is removed to the negative electrode chamber, while H^+ generated in the positive electrode chamber comes into the central channel to make HX (X^- typically being OH^-, HCO_3^-, $^1/_2\ CO_3^{2-}$, $B(OH)_4^-$, etc.). The suppressor explicitly accomplishes *quantitative* exchange of MX to HX. Indeed, it is critical that it does so because the detection limits are directly related to the stoichiometric completion of the exchange process.[33] In suppressor use, quantitative ion exchange is essential for the reproducibility of performance. Suppressors have evolved from packed columns to chemically regenerated membrane devices, to electrodialytic units. But the need to achieve stoichiometric exchange has not changed. Current electrodialytic suppressors operate with 80−90% Faradaic efficiency.[34] Overdriving such suppressors does not lead to lower background conductance but generates greater noise and reduces lifetime; certain amphoteric analytes can also be lost in an overdriven suppressor.[35]

For strong acids and bases used most commonly as eluents in present-day IC, subquantitative exchange would not lead to a buffer. But for other eluents like $NaHCO_3/Na_2CO_3$ or $Na_2B_4O_7$, subquantitative exchange would lead to buffers, albeit only alkaline buffers would be possible. These eluents are typically used in low millimolar concentrations, substantially lower than typical buffer concentrations. As exchange occurs, a carbonate or borate eluent gradually become nonconductive. When much of the metal cation has been removed, maintaining either good current efficiency or accurately controlling the extent of exchange becomes difficult. It would otherwise be obvious that if HX is a weak acid and a solution of MX is pumped through a CEM-based suppressor, substoichiometric cation exchange will produce buffers with pH adjustable under electrical control. Whether because of our collective myopic focus solely on quantitative suppression, or the above reasons that make accurate control of substoichiometric exchange difficult, this has never been attempted.

Herein we discuss the operation of electrodialytic membrane suppressors used in IC as electrodialytic buffer generators (EBGs) and their nature and characteristics when so operated.

PRINCIPLES

Suppressor-Based Electrodialytic Buffer Generators. Consider the schematic in Figure 1a. A solution of the fully neutralized Na salt of an *n*-protic acid, Na_nX, is influent into a CEM-based suppressor. The Na^+ is at least partially electrodialytically removed and replaced with H^+. For simplicity, we assume a NaX−HX buffer system; the general scheme is applicable to multiprotic acid−base systems. NaX (C M) flows through the central channel at Q mL/min while a current i mA is made to flow through the system. As long as significant concentrations of ions other than H^+ or OH^- remain to be transported, the efficiency of present suppressors can be taken to be Faradaic. With F being the Faraday constant, at steady state, $0.06i/F$ mol/min of Na^+ is removed from the center to the cathode compartment. An equal amount of H^+ from the anode compartment is concurrently introduced to the center. This amounts to HX formation equal to $60\ i/FQ$ M in the center channel while the NaX concentration drops to $C - (60\ i/FQ)$ M. Neglecting activity corrections for the moment, the pH is then simply computed from the familiar Henderson−Hasselbalch equation as

$$\mathrm{pH} = \mathrm{p}K_a + \log\,(CFQ - 60i)/60i \qquad (1)$$

This is usable in the range when an appreciable amount (e.g., > 5%) of HX has formed but also an appreciable amount of NaX remains (and $[Na^+]$ still remains $\gg[H^+]$). At low pH, if $[H^+]$ in the central channel becomes comparable to $[Na^+]$, we can no longer assume that Na^+ transport is the sole Faradaic process. Also, at high [HX] values, HX can be lost through the ion-exchange membranes because uncharged molecules can be freely transported through such membranes. However, transport of a neutral species is not affected by the electric field. The transport is solely driven by the concentration difference and in most cases the magnitude is small. Buffer systems based on multiprotic acids/bases can also avoid such losses. For example, if C M Na_3PO_4 or trisodium citrate is introduced into the system, current-controlled H^+−Na^+ exchange can create an adjustable pH buffer system. There will be no loss of the neutral acid until significant amounts of the free acid form at the high end of the exchange. For the general case of introduction of the C M solution, a fully neutralized salt (M_nX) of an *n*-protic acid (H_nX) being introduced into the system, the charge balance equation is

$$\left(nC - \frac{60i}{FQ}\right) + [\mathrm{H}^+] - \frac{K_W}{[\mathrm{H}^+]} - pC\sum_{p=1}^{n}\alpha_p = 0 \qquad (2)$$

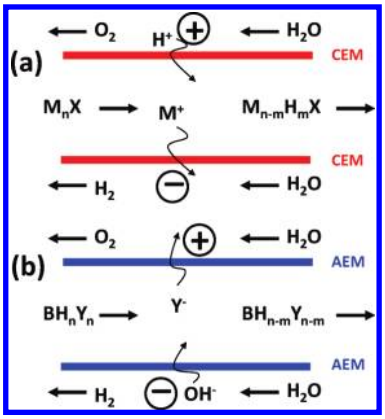

Figure 1. EBG scheme with (a) an anion suppressor (a dual CEM device) with the strong base salt of a multiprotic acid as the feed solution and (b) a cation suppressor (a dual AEM device) with the strong acid salt of a multiprotic base as the feed solution. The drive current controls how much of the strong base cations in panel a and the strong acid anions in panel b are respectively removed from the system to attain the desired pH.

dx.doi.org/10.1021/ac2023712 |*Anal. Chem.* 2012, 84, 67–75

where the first term indicates the remaining M^+ concentration and α_p indicates the fraction of the total anion that exists with a charge of $p-$. The general procedure for solution, including activity corrections, is given in the Supporting Information.

Considerations of an EBG based on a weak base and its salt are similar. Consider a base B that can take up to n protons. A solution of the fully neutralized salt BH_nY_n is influent into an AEM-based suppressor. Some (or all) of the Y^- is removed through the AEM to the anode compartment, while an equal amount of OH^- enters from the cathode compartment to neutralize H^+ (Figure 1b). For the simple case of a monoacidic base B and its salt BHY, eq 1 still applies with K_a being the acid dissociation constant of BH^+ and the sign of the log term reversed:

$$\mathrm{pH} = \mathrm{p}K_a - \log\left(CFQ - 60i\right)/60i \qquad (3)$$

The use of a multiprotic base will avoid loss of the free base and the applicable equation will be similar to eq 2.

A suppressor-based EBG has the advantage that the device is commercially available, and many commercial ICs already allow current programming of the suppressor. In principle, no gas is evolved in the fluid channel of interest. A constant buffer ion concentration is maintained while pH is adjusted by controlling the removal of the counterion with applied current. The approach can thus be thought of as subtractive. While a strong base cation or a strong acid anion is removed from the central channel, H^+ or OH^- (as appropriate) comes in and takes its place to maintain the charge balance. It is interesting to note that the system is not operationally symmetric: It is possible to have an Na_2HPO_4 influent and render it into NaH_2PO_4 quite effectively and efficiently by removing Na^+ and replacing it with H^+. But it is not possible to as easily convert NaH_2PO_4 into Na_2HPO_4. If we electrodialytically introduce Na^+ in the central compartment from a Na^+ source in the anode compartment; an equal amount of Na^+ will be concurrently lost from the center to the cathode compartment, resulting in no net change in the center. However, this does not mean that, with a CEM suppressor-based EBG, a pH profile that increases with time is not possible. One can start with influent Na_3PO_4 and a high suppressor current whence much of the sodium is removed, resulting in an acidic $NaH_2PO_4-H_3PO_4$ buffer. To create an increasing pH profile with time, the suppressor current is correspondingly decreased.

EXPERIMENTAL SECTION

Reagents. All chemicals were commonly available reagent-grade, and distilled deionized water was used throughout. See Supporting Information.

Electrolytic Buffer Generators. ASRS Ultra II and CSRS Ultra (both 4 mm, www.dionex.com) were used as EBGs. Electrolyte solutions were delivered by an ICS2000 IC pump through the eluent channel; water was peristaltically pumped (Gilson Minipuls 2) through the regenerant channels. The suppressor current was software-programmed (Chromeleon V.6.60). The conductivity of the generated buffer solutions is much higher than those addressable by IC conductivity detectors. We therefore prepared high cell constant (6400 cm^{-1}) flow-through detection cells (two tubular electrodes separated by a spacer tube) coupled to a Dionex CD25 conductivity detector. The pH was measured after two-point calibration with standard buffers. Because of concern that the applied voltage, either in the EBG or the preceding conductivity detector, may affect in-line pH measurement, most of the initial pH measurements were made by applying constant current steps and collecting the device effluent in discrete aliquots. Since monitoring the results of a programmed current profile was not practical this way, a long narrow-bore tube was connected between the conductivity cell and the home-built pH flow cell. Experiments established that there is no difference between the in-line measured pH and the pH of the collected aliquots. pH was measured in-line henceforth. However, the residence volume between the conductivity and the pH electrode flow cells, the volume of the latter, and the response time of the pH electrode were all significant. All contributed to a slower pH response compared to the conductivity response.

Removal of Microbubbles. Although no gas is formed in the central channel, much gas is formed in the outer channels, especially at high operating currents. The central channel liquid thus becomes saturated with the electrolytic gas (which readily permeates the membranes). In the absence of significant backpressure, microbubbles are formed in the detectors. The frequency of such bubbles predictably increased with applied electrodialytic current. An example is shown in Figure S1 in Supporting Information. We chose therefore to remove the gas from the central channel. Gas collection with a tubular porous membrane was first described 25 years ago[36] and removal of gases by the reverse process shortly thereafter.[37] We presently used a commercially available carbon dioxide removal device (CRD-200−4 mm, Dionex) immediately after the EBG, with both of the external jacket (regenerant) inlet/outlets of the CRD tied in common by a tee and connected to house vacuum (~180 Torr). While the CRD[38,39] is designed for dissolved CO_2 removal, with vacuum applied, it can remove dissolved gas as well as discretely present gas bubbles.

RESULTS AND DISCUSSION

Behavior of a Phosphate EBG. Figure 2 shows the measured effluent pH (●, left ordinate) for a CEM suppressor system with 68 mM Na_3PO_4 as feed. The current versus effluent pH profile exactly reflects the plot for a coulometric titration, which it really is. Rather than a fixed solution volume, there is a constant flow rate; hence the appropriate control variable is current rather than charge.

We also theoretically estimated the pH. Details are given in the Supporting Information. Briefly, the following sequence was used: (a) estimate the ionic strength (I) of the solution; (b) compute individual ion activity coefficients from the Davies equation;[40] (c) for each applicable constant, compute the applicable equilibrium constants in terms of concentrations; (d) express individual ionic concentrations based on these constants and H^+; (e) solve the relevant charge balance equation that contains all ions in solution for H^+ by use of Microsoft Excel Solver; (f) compute all ion concentrations; (g) cycle through a−f until convergence; (h) calculate the activity coefficient of H^+, a_{H^+}, and activity-based pH. The theoretically calculated pH is represented as a solid gray line; it is slightly higher throughout the alkaline pH range compared to the measured pH values. This difference is ascribed to discrete collection and measurement in room air and consequent exposure to CO_2. On the other hand, at the low-pH end, the theoretically computed pH values fall below the experimental values. While the negatively charged membranes effectively inhibit the loss of negative ions, there is no

dx.doi.org/10.1021/ac2023712 |Anal. Chem. 2012, 84, 67–75

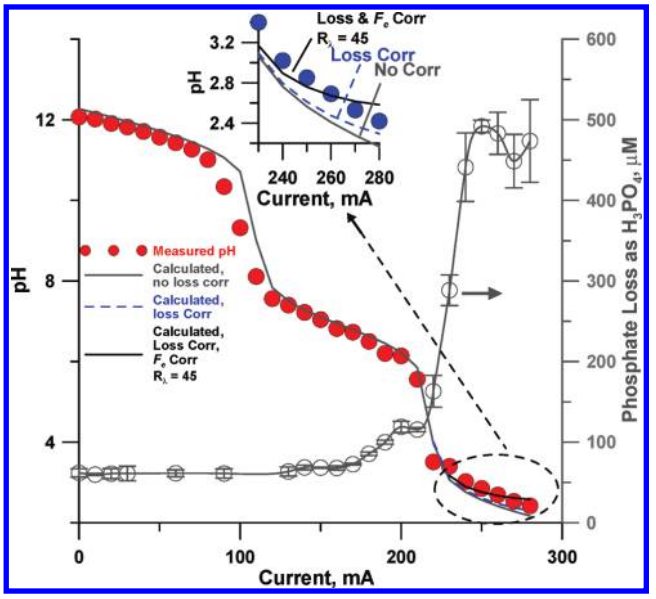

Figure 2. pH as a function of applied current for 68 mM Na_3PO_4, CEM suppressor (ASRS Ultra II (4-mm) 1 mL/min. (○, right ordinate) Concentration of total phosphate lost through the membranes determined by IC analysis of the outer channel effluent. Triplicate injections, ± 1 standard deviation is shown as an error bar. The bottom right is shown in magnified form in the inset. The lines in the pH traces indicate computed values. See text for an explanation for the different computations.

barrier toward the loss of uncharged H_3PO_4. The amount lost was measured by IC and is shown in terms of the central channel concentration (○ with error bars) in Figure 2 (right ordinate). Note that the highest loss (lowest pH) amounts to 0.7% of the total phosphate, not a large amount. Also, this occurs at the extreme end where phosphate is not likely to be used as a buffer. In a suppressor, the two outer electrode channels are fluidically tied together; it is not possible to experimentally determine via which membrane the loss primarily occurs. However, logically it must be primarily through the anodic membrane. The PO_4^{3-} is directed electrically to this membrane and the H^+ generated keeps the membrane in H^+ form. Therefore H_3PO_4 must be formed as a thin layer at the internal surface of the membrane. The pattern of the loss is consistent with this view: the loss is low and essentially constant over a large current range and then starts increasing as $H_2PO_4^-$ begins to be titrated to H_3PO_4 in the final step and H_3PO_4 begins to be formed in significant concentration in the bulk solution. Incorporating this loss of H_3PO_4 into our computations (blue dashed line) makes a difference only at the lowest pH end and brings the theoretical values closer to the measured values, but the computed values still remain lower than the measured values.

Another factor to be considered at low pH is that the Faradaic efficiency (F_e) for Na^+ transport must fall below unity. In a CEM-based suppressor, current is carried by all cations, both Na^+ and H^+. When $[H^+]$ is no longer negligible relative to $[Na^+]$, the fraction of the current carried by Na^+ or F_e will be given by:

$$F_e = \frac{\lambda_{Na^+}[Na^+]}{(\lambda_{Na^+}[Na^+]) + (\lambda_{H^+}[H^+])} = \frac{1}{(1 + R_c R_\lambda)} \qquad (4)$$

where λ_i is the equivalent conductance (proportional to ionic mobility) of ion i; R_c and R_λ are, respectively, the concentration ratio and the mobility ratios of H^+ and Na^+. The infinite dilution R_λ value in solution, 6.98, is readily computed from known values for λ_{Na^+} and λ_{H^+}. This provides at least a first approximation value to use in the computation; the exact F_e value is also dependent on the selectivity coefficient (that governs membrane uptake) and relative transport speeds in the membrane. Available evidence[41] suggests that, in the membrane itself (which may be the limiting element), the mobility ratio of H^+ to Na^+ may be much greater than in free solution. In either case, the applicable form of eq 2 is

$$\left(nC - F_e\frac{60i}{FQ}\right) + [H^+] - \frac{K_W}{[H^+]} - pC\sum_{p=1}^{n}\alpha_p = 0 \qquad (5)$$

Using nonunity F_e that results from a R_λ value of 7, we calculated the theoretical pH values. These values were numerically higher than those which took only H_3PO_4 loss into account. But the difference was too small to be discerned in the scale of Figure 2, even in the magnified inset view of the low-pH end, and hence was not plotted. However, if we keep increasing R_λ values, agreement at the low end pH keeps getting better (note that this correction has no effect on pH ≥ 4) but by the time R_λ is made 45 (plotted as solid black line, see Figure 2 inset), one is perceptibly overcorrecting relative to the lowest measured pH. We conclude that nonunity F_e plays a role that is of significance only at the near-quantitative exchange end; this is of limited interest in buffer generation applications.

Reproducibility and Response Time. Figure 3 shows both conductivity and pH traces for a programmed ascending and descending step current gradient for the same phosphate system over four cycles. The system does exhibit some hysteresis. The membranes have significant ion-exchange capacity and their ionic status depends on previous history and current flux. This creates a difference between the same current steps on ascending versus descending profiles. Details are given in Tables S1 and S2 in the Supporting Information. However, absolute conductance values at either ascending or descending current steps are repeatable (0.30−0.43% RSD, average 0.36% RSD), the conductance values being slightly (0.14−0.38%) but perceptibly higher with ascending than with descending current steps. Similar results are observed for pH: pH values for ascending steps are slightly (0.05−0.10 unit) higher and the reproducibility within each type of step is within 0.005−0.05 pH unit. Response times to step changes in current were calculated from the conductivity detector response (as the pH electrode response is slower). The response time depends on the status of the membrane. In ascending current steps, conductivity decreases and the 90−10% fall times for 0−40, 40−80, 80−120, and 120−160 mA steps were 2.54 ± 0.27, 2.07 ± 0.09, 1.60 ± 0.07, and 0.95 ± 0.03 min, while the 10−90% rise times for 160−120, 120−80, 80−40, and 40−0 mA steps were 0.68 ± 0.06, 0.92 ± 0.15, 2.12 ± 0.05 and 3.43 ± 0.10 min, respectively. The response is clearly faster at high currents when much of the membrane is in the more labile H^+ form. The response is also faster during descending current steps, which calls for less transport through the membrane. This suggests that the primary process that limits the response time is transport through the membrane. The response time is thus faster when the current step is smaller, as in the case of generating a pH gradient over several minutes where the current change is small with time. Detailed results are given in Figure S2 and Tables S3 and S4 in Supporting Information for a current step of 2 mA (104 ⇔102 mA) for the same system. In this case, the respective 90−10% fall and

dx.doi.org/10.1021/ac2023712 |Anal. Chem. 2012, 84, 67–75

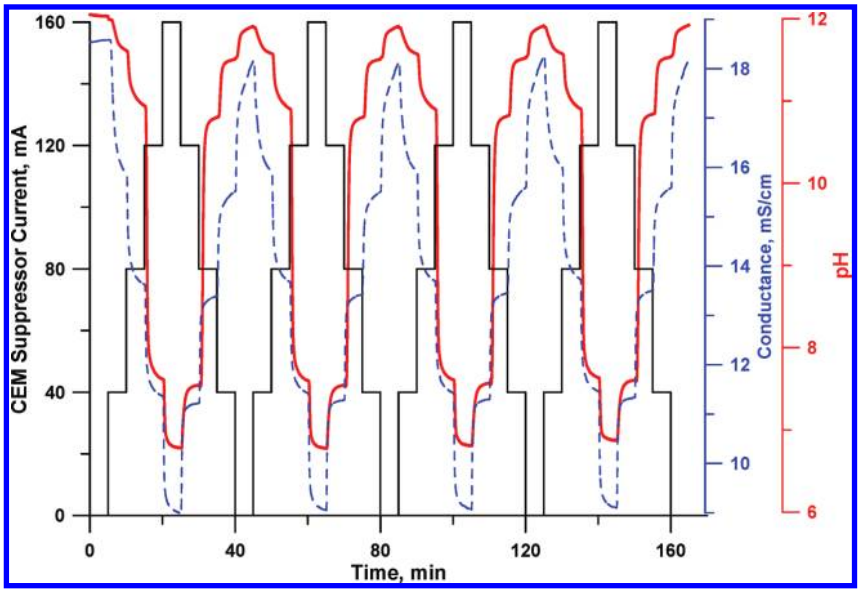

Figure 3. Step gradient response. Four cycles are shown for a Na_3PO_4 feed CEM suppressor system with an influent flow of 1 mL/min. Current steps are 0 → 40 → 80 → 120 → 160 → 120 → 80 → 40 → 0 mA (solid black). pH response is in the thicker line (solid red), and conductivity response is the dashed line (blue).

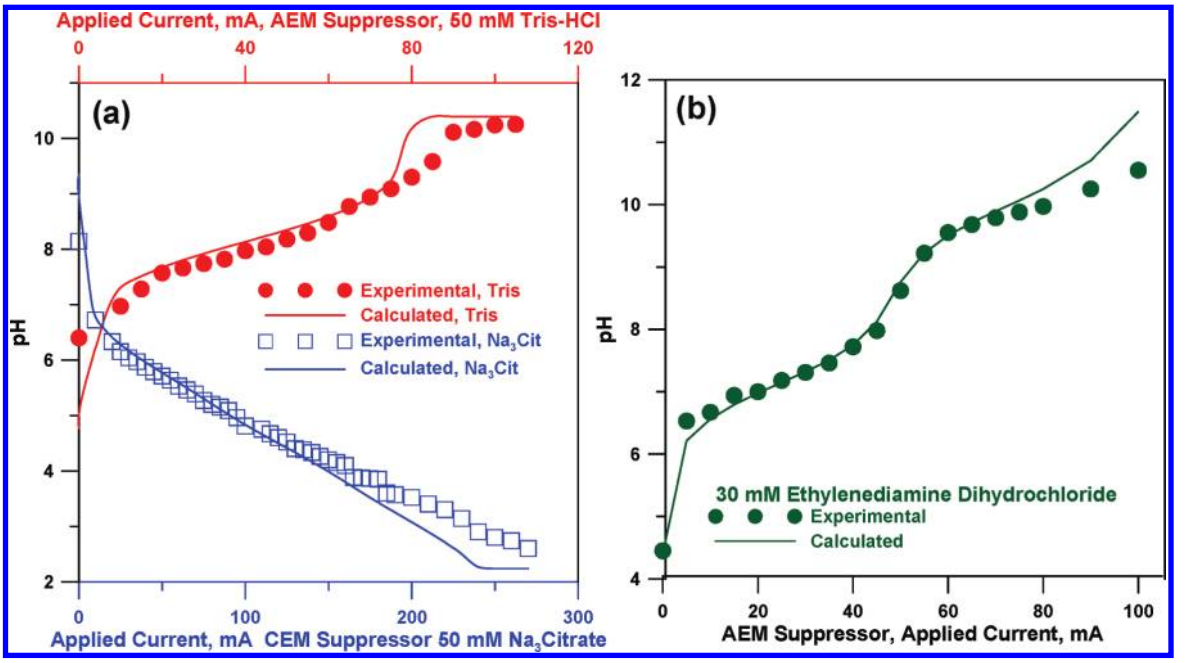

Figure 4. pH as a function of drive current for (a) 50 mM trisodium citrate as the feed solution (ASRS Ultra II, 4 mm) and 50 mM Tris-HCl (CSRS Ultra, 4 mm), and (b) 30 mM ethylenediamine dihydrochloride (CSRS Ultra, 4 mm), all at 1.00 mL/min. Solid lines represent computed pH values; see text.

10−90% rise times for the conductance signals were lower and were more comparable to each other. They ranged from 0.61 to 1.41 and 0.72 to 1.85 min, respectively. A 3-D plot of the results of this experiment is shown as the abstract graphic.

Other Buffers. Figure 4a shows results for 50 mM trisodium citrate as the influent solution with the same CEM-based suppressor system. Since citric acid has three closely spaced pK_a values (3.13, 4.75, and 6.40), individual titration steps are not observed; rather, a nearly linear gradient in pH (from 6.5 to 3) is seen. Citric acid is a substantially larger molecule than H_3PO_4. Since the loss of phosphate through the membrane was small and hardly affected the calculated pH, we did not measure citric acid loss and calculated the pH without assuming any loss. It can be observed that the measured pH begins to significantly deviate from the computed values only below a pH of ~3.5.

Also in Figure 4a is the behavior of a Tris-based buffer system with an AEM-based suppressor system. With a pK_a of 8.1, Tris provides useful buffering in the biologically important buffering range of 7−9. Loss of Tris as a free base was not measured. The computed pH of the initial solution is lower than the observed

dx.doi.org/10.1021/ac2023712 |*Anal. Chem.* 2012, 84, 67−75

value. The commercial product that we assumed to be the pure hydrochloride likely contains a small amount of the free base. Thereafter the computed and the observed values of pH agree well up to pH ~9 (current ~200 mA). The point at which the theoretical and observed values begin to differ is where the last of the Cl^- is removed: the observed values show a much more gradual transition than the sharp change theoretically predicted. The calculation does not take into account any intrusion of dissolved CO_2 from the outer compartments to the center or during collection and measurement.

The two respective pK_a values of the ethylenediammonium ion are 6.85 and 9.93. Both titration steps are observed; the computed pH values again agree with the observed pH over much of the useful buffering range (Figure 4b). This establishes that the principle is equally applicable to multiprotic cationic (basic) buffer systems.

Electrodialytic Generation of a Large Range Linear pH Gradient. Leithe[42] was the first to devise "linear buffers"[43,44] for "single point titrations". The idea was to determine the concentration of a strong acid or strong base by simply adding an aliquot of it to a fixed volume of the "linear buffer" and measuring the pH change. The buffer composition is such that the pH change is linearly related to the amount of the acid/base added. Polyprotic acid−base buffering systems and mixtures thereof have been both theoretically and experimentally studied for the purpose.[45] At least two "polybuffers" based on polyampholytes that accomplish this over a limited pH range are commercially available[46] (these are expensive: present cost is >$1/mL). Efforts to develop buffer compositions with multiple low MW species are given in a number of the papers cited in the introductory discussion on chromatofocusing. pH gradients are also of interest in high-throughput pK_a measurement.[47] In both cases, a linear pH gradient is desired. Mostly, relatively limited pH range gradients with limited linearity have been demonstrated. In flow applications, including chromatography, a further desired requirement is to maintain a constant flow rate for a binary component mixture. Otherwise, minimally a ternary gradient, which includes a diluent, will be needed. Box et al.[47] mixed two solutions, each consisting of six components, to achieve a linear gradient. Although data were not shown for the (linear) composition change versus actual pH, between pH 3 and 11.6 the linear r^2 value between the computed and measured pH was stated to be 0.99.

Any buffer produced by an EBG driven by a linear current gradient is unlikely to produce a linear pH gradient, unless previous "linear buffer" compositions are adopted. Otherwise one ends up revisiting the same composition−computation experimentation−pH measurement optimization steps common to previous efforts. A constant buffer capacity accompanying a linear pH gradient is a great attribute. But is it really needed for chromatography? What is needed is a buffer capacity sufficient to withstand a change in pH (within specified tolerance limits) when the analyte is added at any point in the gradient. For analytical-scale chromatography, this does not necessarily imply a large buffer capacity. Buffer capacity that may vary during a pH gradient is not therefore a major limitation.

To achieve a linear pH gradient, we picked several common buffering agents with pK_a values spread across the range of interest. Phosphoric, citric, and boric acids together provide pK_a values of 2.10, 3.13, 4.75, 6.40, 7.20, 9.24, and 12.38. This potentially covers a large pH range of 2−12 with somewhat of a gap between 9.24 and 12.38. This shortcoming can perhaps be partially addressed by increasing the borate concentration. The change in pH upon incremental removal of K^+ from a mixture containing 15 mM K_3PO_4, 15 mM tripotassium citrate, 11.25 mM $K_2B_4O_7$, and sufficient KOH to adjust the pH to 12 was computed (see Supporting Information). The last two components, equivalent to ~45 mM $KB(OH)_4$, provide 3× the buffer capacity compared to the final neutralization step of 15 mM Na_3PO_4. The same system was also experimentally studied with a staircase current gradient (t = 0−120 min, i = 0−300 mA; Δt = 2 min, Δi = 5 mA). From applying a current step to the observed onset of the pH response required ~0.45 min. After accounting for this time lag, the pH data were averaged over 2 min increments and are plotted in Figure 5a as the black solid line. The computed pH either (i) ignored the possibility of nonunity F_e (red dashed line) or (ii) incorporated nonunity F_e calculated with an R_λ value of 15 (the dilute solution R_λ value for K^+ and H^+ is ~4.76) (blue dashed line). The two differ only at the complete exchange end. Even for a complex system, the relatively simple computation provides pH values close to the measured values. Knowing the behavior of the current versus pH makes it simple to generate a substantially more linear pH gradient against time and also eliminate the wasted time near the end of the run where pH decreases only slowly. A single iteration of the original uniform current steps (red) to that suggested by the current−pH behavior produces the results in blue (Figure 5b; see Supporting Information for the algorithm used for iteration). Since the time steps are still obviously too long, reducing time steps to 0.5 min and a further iteration of the current program to improve linearity produces the results in Figure 6. Figure 6 actually contains three overlaid traces of the generated pH profile, indicating excellent reproducibility. Among the triplicate set of 7500 time versus pH points, the maximum variance was 0.70% (average 0.20 ± 0.14% RSD). While there are minor deviations that can still be improved on, our present hardware/software combination did not allow better than 1 mA resolution in current. This is easily improved. Nonuniform time steps were also possible but were eschewed because of additional complexity. The linearity of the gradients (pH vs time) exhibited r^2 values of 0.9996, 0.9996, and 0.9997 from a pH range of 11.9−3. To manipulate the experimental pH to whatever desired form (linear, convex, concave), it must be obvious that it is much easier to reprogram a current profile than to alter solution compositions or mixing ratios of multiple components. In principle, software that iteratively achieves any desired profile could be relatively easily set up.

Maintaining a Relatively Constant Ionic Strength. Figure 5a also shows the computed ionic strength profile that decreases continuously as the pH decreases. This may not be desirable. To maintain the ionic strength nearly constant, an indifferent salt, for example, NaCl, present at a significantly higher concentration than that of the buffering species can be used. Aside from maintaining a near-constant ionic strength, this has the added advantages that (a) F_e will never have a nonunity value and (b) the buffer can have both cationic and anionic buffering components, for example, *n*-butylamine,[44] pK_a 10.61, can be added to our previous phosphate−citrate−borate mixture to better fill the pK_a gap in this region. In the absence of large concentrations of NaCl, we would have lost the butylammonium ($BuNH_3^+$) ion from the system as a cationic charge carrier. But in the presence of a large excess of Na^+, the loss of the much less mobile (especially through the membrane) $BuNH_3^+$ will be insignificant.

Thus, we prepared a mixture of 15 mM each K_3PO_4, tripotassium citrate, and $BuNH_2$ and 3.75 mM $K_2B_4O_7$ with

dx.doi.org/10.1021/ac2023712 |*Anal. Chem.* 2012, 84, 67–75

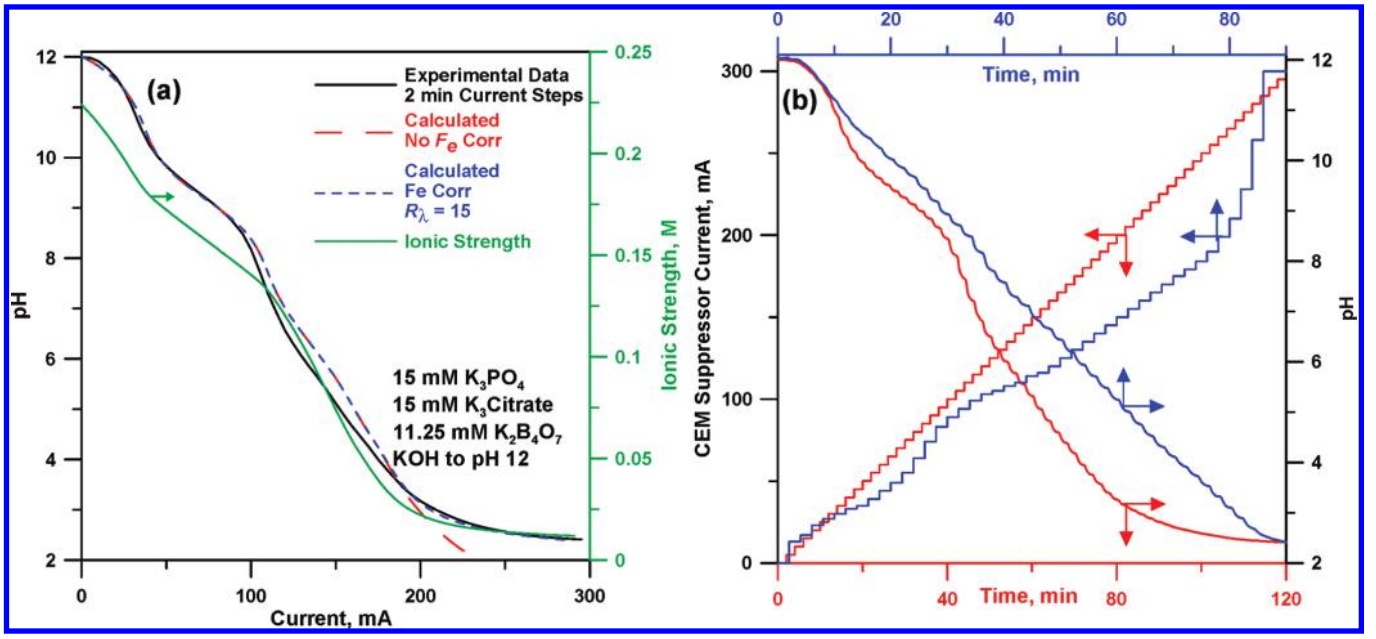

Figure 5. CEM suppressor (ASRS Ultra II, 4 mm), 1 mL/min; feed composition is shown in the inset. (a) Solid black line depicts experimental data obtained with 2 min current steps, the corresponding (time-lag-corrected) 2 min averages for the pH are plotted. The computed values are shown as dashed lines; the blue dashed line takes nonunity Faradaic efficiency (F_e) due to current conduction by H^+ into account. See text. The green line shows the ionic strength (right ordinate). (b) Red traces, bottom abscissa: 2 min uniform 5 mA current steps generate the pH profile that appears in 2 min averaged version in panel a. Blue traces: learning from the observed profile in red, a substantially linear gradient is generated by use of nonuniform current steps.

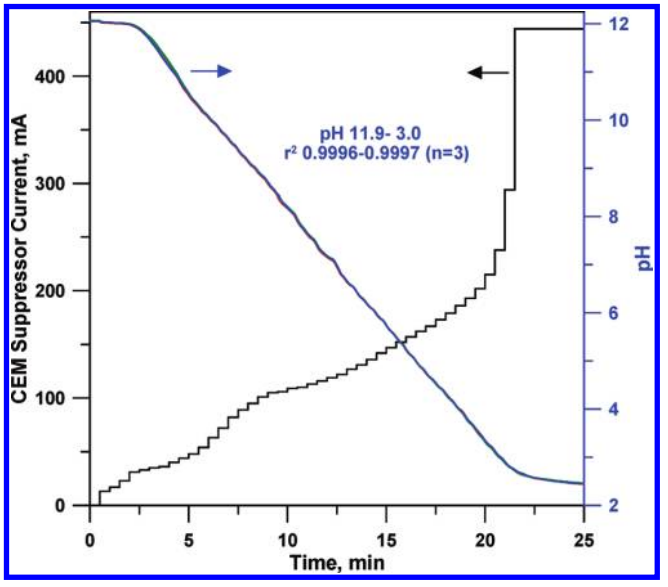

Figure 6. Three repeated 25 min linear pH gradient runs overlaid (right ordinate); the current program uses the left ordinate.

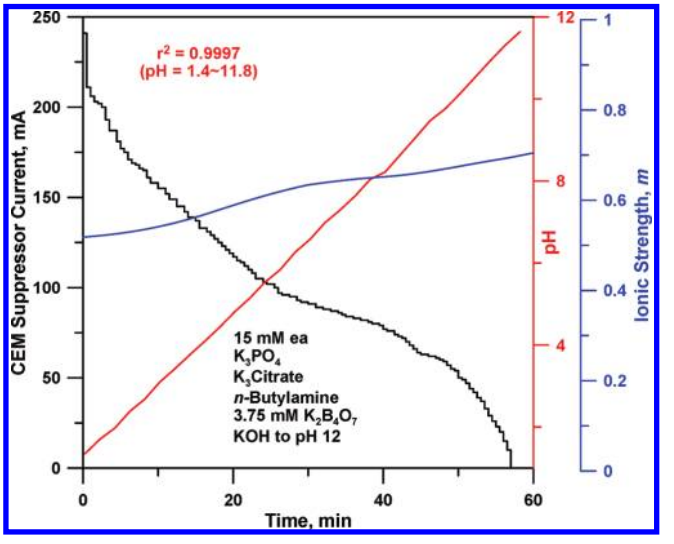

Figure 7. A four-component buffering mixture with an increasing linear pH gradient in the presence of large amounts of NaCl. Without the presence of the salt, the ionic strength will change by more than an order of magnitude (see Figure 5a).

0.5 M NaCl added. Computations used the known mean ionic activity coefficient (0.680) of a 0.5 *m* NaCl solution.[48] Single ion activity coefficients were calculated therefrom, noting the charge and size dependence. Both computed and experimental results are shown in Figure 7. Note that since F_e remains unity throughout, the buffer capacity at any point is essentially the reciprocal of the slope of the pH versus drive current plot. Herein we have used a descending current gradient to demonstrate the capability of a CEM-based suppressor to generate a temporally increasing pH profile; the accompanying change in ionic strength is relatively minor.

In summary, we have demonstrated the principles and practice of generating pH buffers electrodialytically with commonly available suppressors for IC. While present suppressors will not support pressures high enough to locate the device on the high-pressure side of a pump, ion-exchange bead-based devices that tolerate much higher pressures have already been described.[49−52] Such devices can be readily constructed in an array format. With a

dx.doi.org/10.1021/ac2023712 |*Anal. Chem.* 2012, 84, 67−75

ternary gradient system, an organic solvent gradient can be incorporated without a change in buffer ion concentration. To generate an additional gradient in ionic strength/salt beyond that resulting from pH change, a further pumping channel (to add variable amounts of salt) will be needed.

It is also clear that suppressors can be used as flow-through coulometric ion removal devices. This property can be readily exploited as a process titrator, especially in conjunction with rapid triangular wave current sweeps as previously reported.[53,54] For sample streams that can flow through the suppressor, an AEM-based suppressor can be used to remove anions, introduce OH^-, and titrate an acidic stream while a CEM-based suppressor can be used to remove cations, introduce H^+, and titrate a base. For streams that are not compatible to directly flow through the suppressor, salt solutions flowing through a CEM/AEM suppressor can generate the titrant acid/base, respectively, in a current-controlled mode to be added to the sample stream.

Even in a purely aqueous system, it is not possible to independently control both pH and ionic strength with a suppressor-based EBG, especially when the ionic strength is controlled by the buffering species. This is possible with a different, additive electrodialytic membrane device that is described in the accompanying paper.[55]

■ ASSOCIATED CONTENT

Supporting Information. Additional text with 23 equations, two figures, and four tables (pdf) and one spreadsheet (xls) as described in the text. This material is available free of charge via the Internet at http://pubs.acs.org.

■ AUTHOR INFORMATION

Corresponding Author
*E-mail: Dasgupta@uta.edu.

■ ACKNOWLEDGMENT

This work was supported by the National Science Foundation through CHE-0821969 and by Thermo Fisher Scientific (formerly Dionex Corporation). We thank Christopher A. Pohl.

■ REFERENCES

(1) Li, Y.-C.; Wiklund, L.; Tarkkila, P.; Bjerneroth, G. *Resuscitation* **1996**, *32*, 33–44.
(2) Kang, J.; Ramu, S.; Lee, S.; Aguilar, B.; Ganesan, S. K.; Yoo, J.; Kalra, V. K.; Koh, C. J.; Hong, Y.-K. *Anal. Biochem.* **2009**, *386*, 251–255.
(3) Fringuelli, F.; Pizzo, F.; Vaccaro, L. *J. Org. Chem.* **2001**, *66*, 4719–4722.
(4) Jacobsen, C. F.; Leonis, J.; Linderstrom-Lang, K.; Ottesen, M. *Methods Biochem Anal.* **1957**, *4*, 171–210.
(5) Einsel, D. W., Jr.; Trurnit, H. J.; Silver, S. D.; Steiner, E. C. *Anal. Chem.* **1956**, *28*, 408–410.
(6) Adams, R. E.; Betso, S. R.; Carr, P. W. *Anal. Chem.* **1976**, *48*, 1989–1996.
(7) Karcher, R. E.; Pardue, H. L. *Clin. Chem.* **1971**, *17*, 214–221.
(8) Kao, L. T. H.; Hsu, H.-Y.; Gratzl, M. *Anal. Chem.* **2008**, *80*, 4065–4069.
(9) Timperman, A.; Tracht, S. E.; Sweedler, J. V. *Anal. Chem.* **1996**, *68*, 2693–2698.
(10) Zhao, F.; Harnisch, F.; Schröder, U.; Scholz, F.; Bogdanoff, P.; Herrmann, I. *Environ. Sci. Technol.* **2006**, *40*, 5193–5199.
(11) Liu, G. *Chromatographia* **1989**, *28*, 493–496.
(12) Cantú, R.; Evans, O.; Kawahara, R. K.; Wymer, L. J.; Dufour, A. P. *Anal. Chem.* **2001**, *73*, 3358–3364.
(13) Wiczling, P.; Markuszewski, M. J.; Kaliszan, M.; Kaliszan, R. *Anal. Chem.* **2005**, *77*, 449–458.
(14) Subirats, X.; Bosch, E.; Rosés, M. *J. Chromatogr. A* **2007**, *1138*, 203–215.
(15) Espinosa, S.; Bosch, E.; Rosés, M. *Anal. Chem.* **2002**, *74*, 3809–3818.
(16) Kaliszan, R.; Haber, P.; Baczek, T.; Siluk, D. *Pure Appl. Chem.* **2001**, *73*, 1465–1475.
(17) Wiczling, P.; Markuszewski, M. J.; Kaliszan, M.; Galer, K.; Kaliszan, R. *J. Pharm. Biomed. Anal.* **2005**, 871–875.
(18) Kaliszan, R.; Wiczling, P.; Markuszewski, M. J. *J. Chromatogr. A* **2004**, *1060*, 165–175.
(19) Kaliszan, R.; Wiczling, P. *Anal. Bioanal. Chem.* **2005**, *382*, 718–727.
(20) Kaliszan, R.; Wiczling, P.; Markuszewski, M. J. *Anal. Chem.* **2004**, *76*, 749–760.
(21) Wiczling, P.; Markuszewski, M. J.; Kaliszan, R. *Anal. Chem.* **2004**, *76*, 3069–3077.
(22) Sluyterman, L. A. A. E.; Elgersma, O. *J. Chromatogr.* **1978**, *150*, 17–30.
(23) Sluyterman, L. A. A. E.; Elgersma, O. *J. Chromatogr.* **1978**, *150*, 31–44.
(24) Andersen, T.; Pepaj, M.; Trones, R.; Lundanes, E.; Greibrokk, T. *J. Chromatogr. A* **2004**, *1025*, 217–226.
(25) Kang, X.; Bates, R. C.; Frey, D. D. *J. Chromatogr. A* **2000**, *890*, 37–43.
(26) Liu, Y.; Anderson, D. J. *J. Chromatogr. A* **1997**, *762*, 47–54.
(27) Liu, Y.; Anderson, D. J. *J. Chromatogr. A* **1997**, *762*, 207–217.
(28) Farnan, D.; Moreno, G. T. *Anal. Chem.* **2009**, *81*, 8846–8857.
(29) Lian, S.; Anderson, D. J. *J. Chromatogr. A* **2001**, *909*, 191–205.
(30) Lian, S.; Anderson, D. J. *Anal. Chem.* **2002**, *74*, 5641–5649.
(31) Strong, D. L.; Dasgupta, P. K. *Anal. Chem.* **1989**, *61*, 939–945.
(32) Haddad, P. R.; Jackson, P. E.; Shaw, M. J. *J. Chromatogr. A* **2003**, *1000*, 725–742.
(33) Tian, Z. W.; Hu, R. Z.; Lin, H. S.; Hu, W. L. *J. Chromatogr.* **1988**, *439*, 151–157.
(34) Liu, Y.; Srinivasan, K.; Pohl, C.; Avdalovic, N. *J. Biochem. Biophys. Methods* **2004**, *60*, 205–232.
(35) Dimitrakopoulos, I. K.; Thomaidis, N. S.; Megoulas, N. C.; Koupparis, M. A. *J. Chromatogr. A.* **2010**, *1217*, 3619–3627.
(36) Dasgupta, P. K.; McDowell, W. L.; Rhee, J.-S. *Analyst* **1986**, *111*, 87–90.
(37) Dong, S.; Dasgupta, P. K. *Environ. Sci. Technol.* **1987**, *21*, 581–588.
(38) Ullah, S. M. R.; Adams, R. L.; Srinivasan, K.; Dasgupta, P. K. *Anal. Chem.* **2004**, *76*, 7084–7093.
(39) Dionex Corporation. CRD carbonate removal device. http://www.dionex.com/en-us/products/accessories/reagents-accessories/crd/lp-73608.html
(40) Christian, G. D. *Analytical Chemistry*, 6th ed.; Wiley: New York, 2003; p 213.
(41) Yeager, H. L. *ACS Symp. Ser.* **1982**, *180*, 41–64.
(42) Leithe, W. *Chem. Ing. Tech.* **1964**, *36*, 112–114.
(43) Johannson, G.; Backën, W. *Anal. Chim. Acta* **1974**, *69*, 415–424.
(44) Åström, O. *Anal. Chim. Acta* **1977**, *88*, 17–23.
(45) Righetti, P. G.; Fazio, M.; Tonani, C.; Gianazza, E.; Celentano, F. C. *J. Biochem. Biophys. Methods* **1988**, *16*, 129–140.
(46) GE Health Care. Polybuffers. http://www.gelifesciences.com/aptrix/upp01077.nsf/content/Products?OpenDocument&parentid=555&moduleid=165538 Accessed November 12, 2011.
(47) Box, K.; Bevan, C.; Comer, J.; Hill, A.; Allen, R.; Reynolds, D. *Anal. Chem.* **2003**, *75*, 883–892.
(48) Hamer, W. J.; Wu, Y.-C. *J. Phys. Chem. Ref. Data* **1972**, *1*, 1047–1100.
(49) Yang, B.; Takeuchi, M.; Dasgupta., P. K. *Anal. Chem.* **2008**, *80*, 40–47.

(50) Yang, B.; Zhang, F.; Liang, X.; Dasgupta, P. K. *J. Chromatogr. A* **2009**, *1216*, 2412–2416.
(51) Yang, B. C.; Chen, Y. J.; Mori, M.; Ohira, S. I.; Azad, A. K.; Dasgupta, P. K.; Srinivasan, K. *Anal. Chem.* **2010**, *82*, 951–958.
(52) Chen, Y.; Mori, M.; Pastusek, A. C.; Schug, K. A.; Dasgupta, P. K. *Anal. Chem.* **2011**, *83*, 1015–1021.
(53) Tanaka, H.; Dasgupta, P. K.; Huang, J. *Anal. Chem.* **2000**, *72*, 4713–4720.
(54) Dasgupta, P. K.; Jo, K. *Electroanalysis* **2002**, *14*, 1383–1390.
(55) Chen, Y.; Edwards, B. L.; Dasgupta, P. K.; Srinivasan, K. *Anal. Chem.* **2012**, DOI: 10.1021/ac2023734 (companion paper).